First measurement of near-threshold J/ψ exclusive photoproduction off the proton: Supplemental Material

(Dated: June 21, 2019)

The total cross-section in bins of beam energy and the differential cross-section as function of $-(t-t_{min})$ are given in Tables I and II together with the statistical and systematic errors for the individual data points. Table III summarizes our estimate of the systematic errors for the overall cross-section normalization.

Energy bin, GeV	σ, nb	stat. error, nb	syst. error, nb
8.2-8.56	0.116	0.031	0.013
8.56-8.92	0.343	0.067	0.082
8.92-9.28	0.313	0.127	0.052
9.28-9.64	0.835	0.194	0.185
9.64-10	0.868	0.196	0.109
10-10.36	0.949	0.187	0.102
10.36-10.72	1.383	0.284	0.323
10.72-11.08	1.274	0.206	0.184
11.08-11.44	2.158	0.421	0.657
11.44-11.8	3.245	0.928	0.384

TABLE I: $\gamma p \to J/\psi p$ total cross-sections, statistical and systematic errors of the individual points in bins of beam energy.

$-(t-t_{min})$ bin, GeV^2	$d\sigma/dt$, nb/GeV^2	stat. error, nb/GeV^2	syst. error, nb/GeV^2
0-0.15	1.643	0.334	0.058
0.15-0.3	1.249	0.265	0.019
0.3-0.45	1.088	0.248	0.012
0.45-0.6	0.627	0.182	0.024
0.6-0.75	0.599	0.163	0.047
0.75-0.9	0.470	0.145	0.006
0.9-1.05	0.400	0.134	0.011

TABLE II: Differential cross-sections, statistical and systematic errors of the individual points in bins of $-(t-t_{min})$.

Origin	Estimate, %
$\varepsilon_{BH}/\varepsilon_{J/\psi}$ relative efficiency	23
Radiative corrections	8.3
TCS contribution to BH	8
ρ' contribution to BH	7
total	26.7

TABLE III: Contributions to the total normalization error added quadratically.

The total cross-section calculated from the SLAC [1] data and shown in Fig. 3 of the paper is given in Table IV.

Energy , GeV	σ, nb	error, nb
13	2.240	0.472
15	3.304	0.560
15	4.312	0.840
16	4.515	0.606
17	5.866	0.543
19	5.750	0.586
19	6.389	0.586
19	7.986	0.532
21	7.667	0.630

TABLE IV: Total cross-section vs beam energy calculated from $d\sigma/dt$ (at $t = t_{min}$) from the SLAC data [1] assuming dipole t-dependence, Eq.(1) $m_0 = 1.14$ GeV in the paper.

In Fig. 1 the GlueX, SLAC, and Cornell results for the total cross-section are compared to the JPAC model curves for the three LHCb pentaquarks separately with branching fractions corresponding to the upper limits as estimated in the paper, when using only the errors of the individual data points.

The results for the upper limits of the pentaquark branching fractions $\mathcal{B}(P_c^+ \to J/\psi p)$ are summarized in Table V.

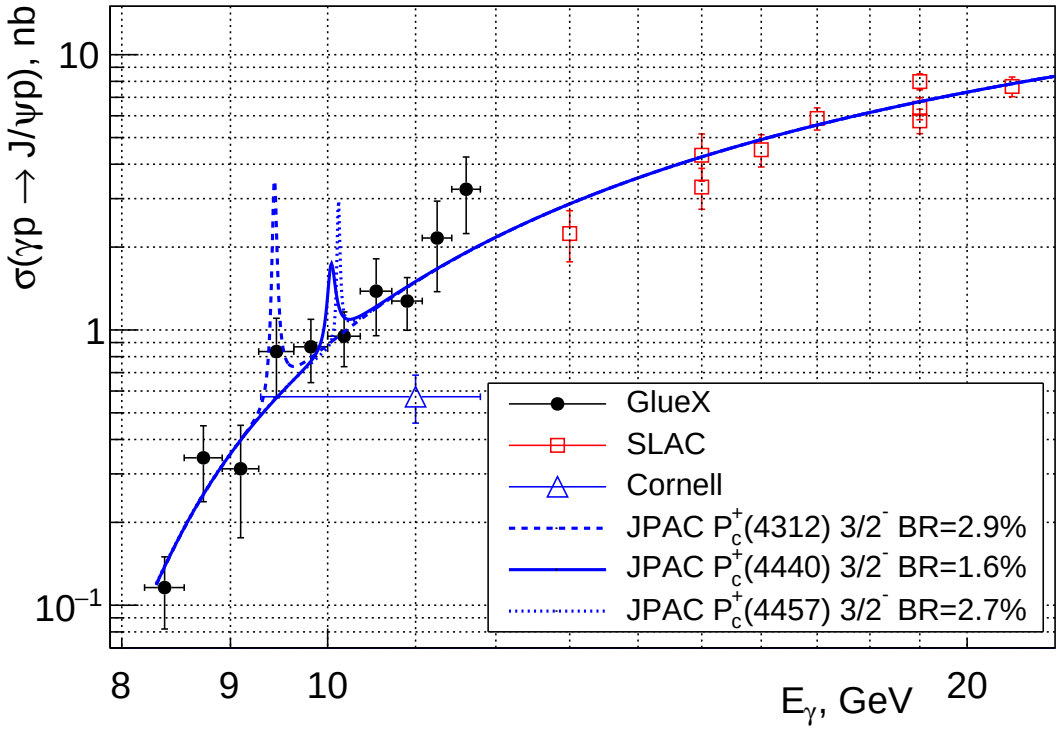

FIG. 1: GlueX results for the J/ψ total cross-section vs beam energy, Cornell [2], and SLAC [1] data compared to the JPAC model [3] corresponding to $\mathcal{B}(P_c^+(4312) \to J/\psi p) = 2.9\%$, $\mathcal{B}(P_c^+(4440) \to J/\psi p) = 1.6\%$, and $\mathcal{B}(P_c^+(4457) \to J/\psi p) = 2.7\%$, for the $J^P = 3/2^-$ case as discussed in the paper.

	$\mathcal{B}(P_c^+ \to J/\psi p)$ Upper Limits, %		$\sigma_{\max} \times \mathcal{B}(P_c^+ \to J/\psi p)$ Upper Limits, nb	
	p.t.p. only	total	p.t.p only	total
$P_c^+(4312)$	2.9	4.6	3.7	4.6
$P_c^+(4440)$	1.6	2.3	1.2	1.8
$P_c^+(4457)$	2.7	3.8	2.9	3.9

TABLE V: Summary of the estimated upper limits for the P_c^+ states at 90% confidence level, as discussed in the paper. Separately shown are the results when using the errors of the individual data points (p.t.p.) only and the total ones that include the uncertainties in the model parameters and the overall normalization.

The tagged GlueX beam energy spectrum, given as an accumulated luminosity, is shown in Fig. 2. It is a result of using both, diamond (dominantly) and amorphous radiators.

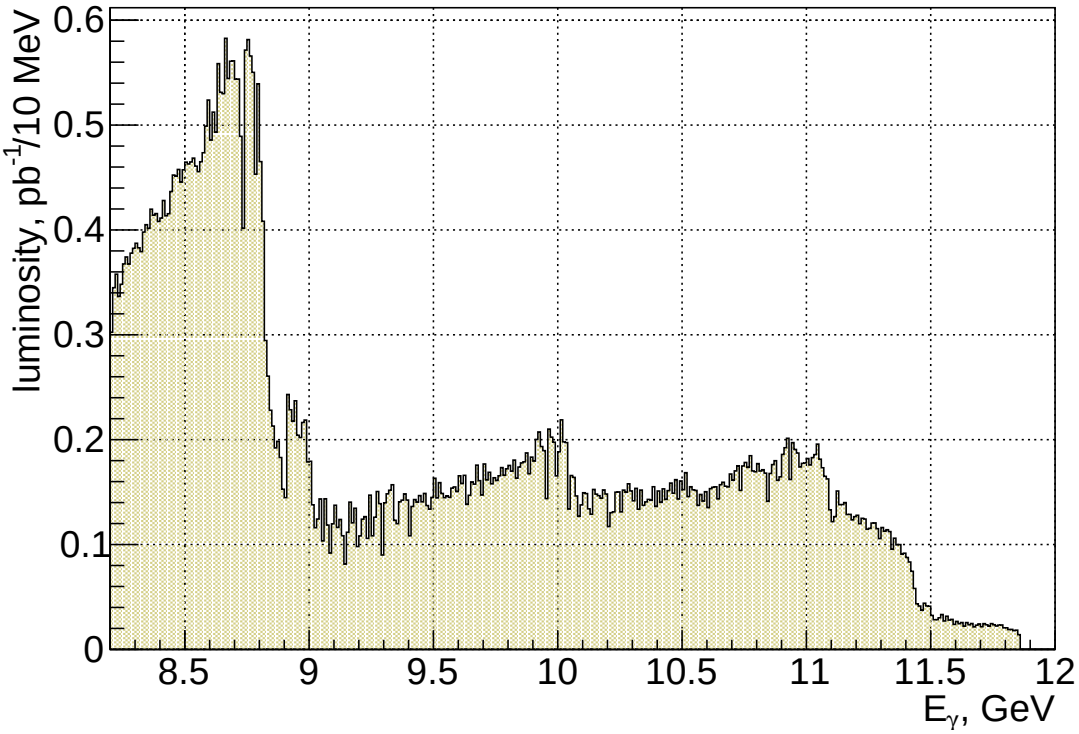

FIG. 2: The tagged photon luminosity as a function of beam energy.

The procedure for extracting the electron/positron BH yield is illustrated in Figs. 3,4. It is applied separately for the two calorimeters (BCAL and FCAL) and in bins of beam energy in order to obtain the final cross section results. The pion contamination varies between between 30 and 60%.

[1] U. Camerini, J. Learned, R. Prepost, C. Spencer, D. Wiser, W. Ash, R. L. Anderson, D. M. Ritson, D. Sherden, and C. K. Sinclair, Phys. Rev. Lett. **35**, 483 (1975).

[2] B. Gittelman, K. M. Hanson, D. Larson, E. Loh, A. Silverman, and G. Theodosiou, Phys. Rev. Lett. **35**, 1616 (1975).

[3] A. Blin, C. Fernandez - Ramirez, A. Jackura, V. Mathieu, V. Mokeev, A. Pilloni, and A. Szczepaniak, Phys. Rev. D **94**, 034002 (2016).

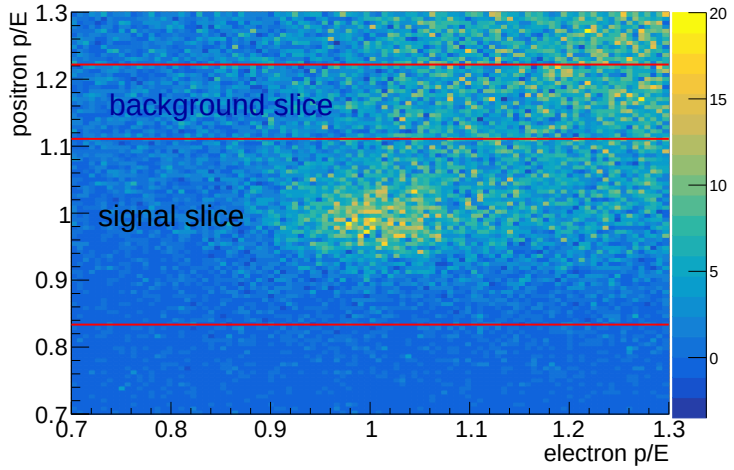

FIG. 3: p/E distribution of the two leptons. The background slice ($2\sigma < p/E - 1 < 4\sigma$ cut on the y-axis), and the slice containing the signal ($-3\sigma < p/E - 1 < 2\sigma$ cut on the y-axis) are indicated with horizontal lines.

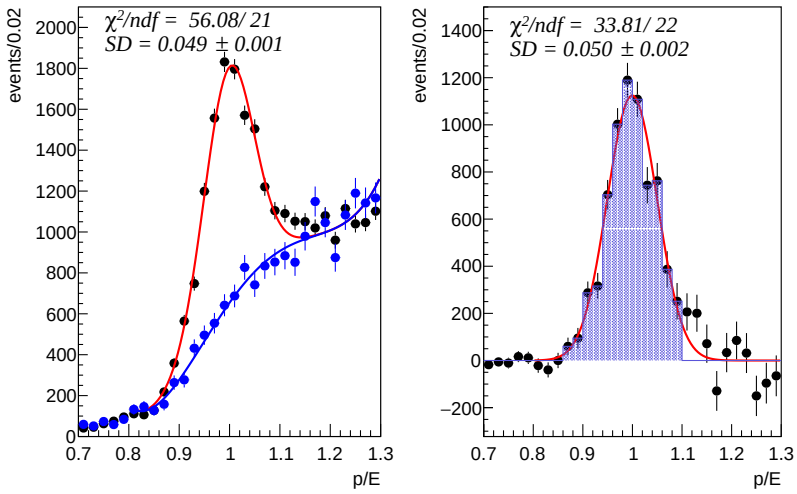

FIG. 4: Left plot: the signal slice from Fig.3 projected on the x-axis (black points) fitted with a background shape times a normalization parameter p_{norm} (blue line) plus a Gaussian (red line); the background shape is a polynomial fit of the projection of the background slice from Fig.3 (blue points normalized by p_{norm}). Right plot: the difference of the black and blue points from the left plot representing the electron/positron signal fitted with a Gaussian. The BH yiled is assigned to the number of events within $(-3\sigma, +2\sigma)$ of the peak (shaded histogram).